

## Abrupt and Defect-Free $p^+-n^+$ Junction Formed by Low-Temperature Photo-Epitaxy with Continuous Boron and Phosphorous Doping

Tatsuya Yamazaki, Hiroshi minakata, and Takashi Ito

*Fujitsu Laboratories Ltd.*

10-1 Morinosato-Wakamiya, Atsugi 243-01, Japan

Heavily doped  $p^+-n^+$  silicon epitaxial layer were continuously grown at 600°C using photo-epitaxy. The surface pits, phosphorous activation ratio, and electrical properties of the heavily phosphorous doped photo-epitaxial layer were greatly improved by the continuous growth on the  $p^+$  photo-epitaxial layer. Hole concentration was above  $1 \times 10^{19} \text{ cm}^{-3}$ , and we obtained device-level crystal quality. The very low growth temperature enabled extremely abrupt impurity profiles of boron and phosphorous.

### Introduction

Impurity doping of epitaxial films is necessary for many device applications. Especially, heavy impurity doping with an abrupt impurity profile is often essential for fabrication of ULSI. In conventional CVD epitaxy, however attempts to obtain abrupt impurity profiles with heavy phosphorous and boron doping have not been successful because doped impurity atoms are diffused due to high growth temperature above 1000°C. Some low temperature epitaxial techniques have been reported, but still do not produce the required device-level crystal quality in the heavy impurity doping region.(1)-(5) We have developed a low-temperature epitaxial technique using direct UV photosensitization of disilane gas.(6),(7) The UV irradiation increases the growth rate, lowers the growth temperature, and enables heavy boron doping with high crystal quality.(8)

This paper describes the heavy phosphorous doping and  $p^+-n^+$  continuous growth in the photo-epitaxy, the resulting crystal quality, impurity profile, and electrical properties.

### Experiment

Low-temperature photo-epitaxy was done in a specially designed quartz chamber having a base

pressure of  $1 \times 10^{-4} \text{ Pa}$  (Fig. 1). A (100) oriented Si wafer was heated by IR lamps from behind. We used high pressure mercury lamps with UV intensity of  $1.2 \text{ W/cm}^2$  as the UV light source. Disilane at 1.5 cc/min was used as the Si source, diborane as the p-type doping source, phosphine as the n-type doping source, and hydrogen at 20 l/min as the carrier gas. Deposition pressure was 27 kPa. The Si wafer was cleaned by conventional wet methods before being loaded into the growth chamber. To reduce the native oxide, the wafer was heated at 900°C for 10 minutes in hydrogen before deposition. The temperature was then reduced to the deposition temperature of 600°C.

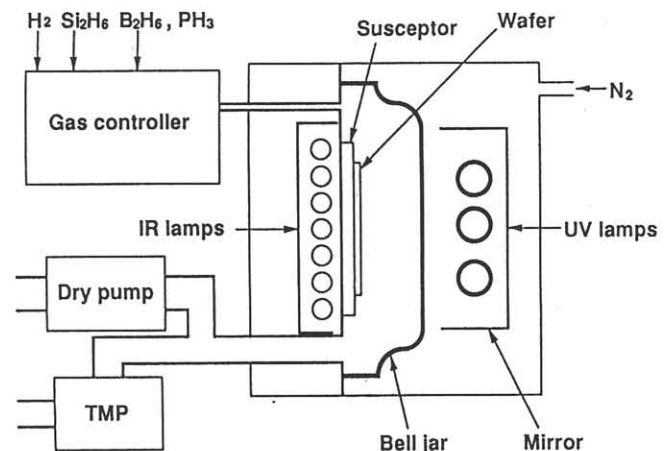


Fig. 1 Experiment set up

## Results and Discussion

### (1) Heavy phosphorous doping in photo-epitaxy

To make the  $p^+-n^+$  junction, heavy phosphorous doping in the photo-epitaxy is necessary. In  $n^+$  photo-epitaxial layer grown on a  $p^-$  substrate ( $\rho = 10 \Omega\text{cm}$ ), the doped electron concentration increased with phosphine flow rate, and saturated at about  $n = 5 \times 10^{18} \text{ cm}^{-3}$  (Fig. 2). Adding more phosphine degraded crystal quality and caused a phosphorous-silicon compound growth. Through the doping range, the doped phosphorous atoms only activated less than 60%, and the electron Hall mobility in the  $n^+$  photo-epitaxial layer was also smaller than that of bulk Si. These results indicate the poor crystal quality of the heavily phosphorous doped photo-epitaxial layer grown on the  $p^-$  substrate.

Heavily phosphorous-doped photo-epitaxial layers grown on the  $p^-$  substrate with a phosphorous concentration above  $1 \times 10^{17} \text{ cm}^{-3}$  had many surface pits (Fig. 3(a)). These surface pits increased as the doping concentration increased, and maximum pit density was at  $10^7 \text{ cm}^{-2}$  above the doped phosphorous concentration of  $5 \times 10^{18} \text{ cm}^{-3}$ . We examined the crystal structure of this defect with TEM (Fig. 3(b)). This defect occurred from the epi-substrate interface, and the origin may be phosphorous precipitation and extraordinary nucleation on the  $p^-$  substrate surface at the initial stage of the  $n^+$  photo-epitaxial growth.

### (2) Continuous growth of $p^+$ and $n^+$ layer

We continuously grew a heavily phosphorous doped photo-epitaxial layer on a heavily boron doped photo-epitaxial layer. Photo-epitaxy can grow a single crystal up to the doped boron concentration of  $1.5 \times 10^{20} \text{ cm}^{-3}$  with perfect activation of doped boron atoms and no crystal defects at  $600^\circ\text{C}$ .<sup>(8)</sup> Using such low-temperature photo-epitaxy, we could grow a  $n^+$  photo-epitaxial layer on a  $p^+$  photo-epitaxial layer by simply changing the doping gas from diborane to phosphine. The  $n^+$  layer was 150 nm thick and  $p^+$  layer was 50 nm thick.

The low growth temperature of  $600^\circ\text{C}$  enabled us to obtain extremely abrupt impurity profiles. The boron and phosphorous profiles of continuously grown  $p^+-n^+$

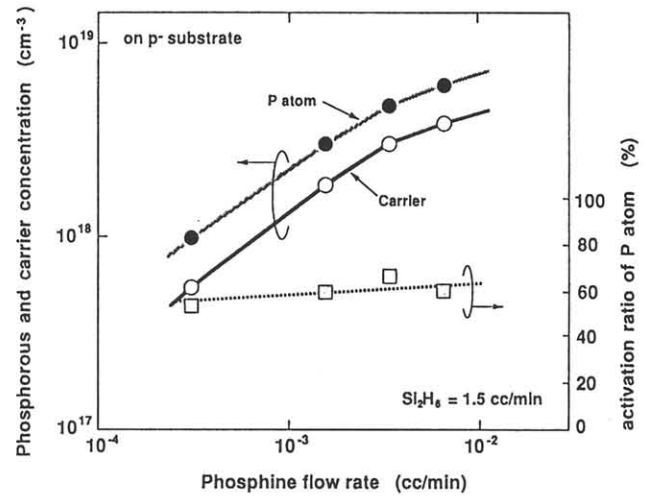


Fig. 2 The phosphine flow rate dependence of the doped phosphorous atoms, doped carrier concentration, and activation ratio of doped phosphorous atoms in the  $n^+$  photo-epitaxial layer grown on the  $p^-$  substrate. The resistivity of the  $p^-$  substrate was  $10 \Omega\text{cm}$ .

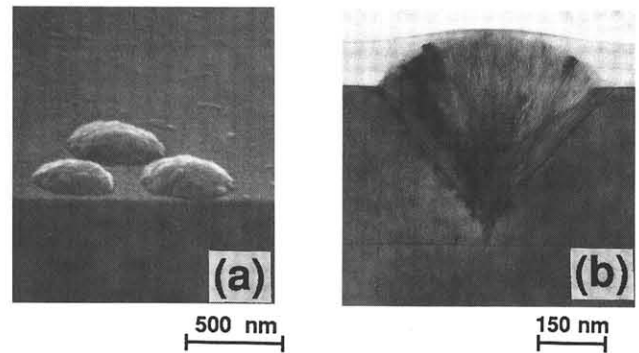


Fig. 3 The surface pits on  $n^+$  photo-epitaxial layer grown on the  $p^-$  substrate. (a) SEM photograph of the surface pits. (b) TEM photograph of the cross section of the surface pits.

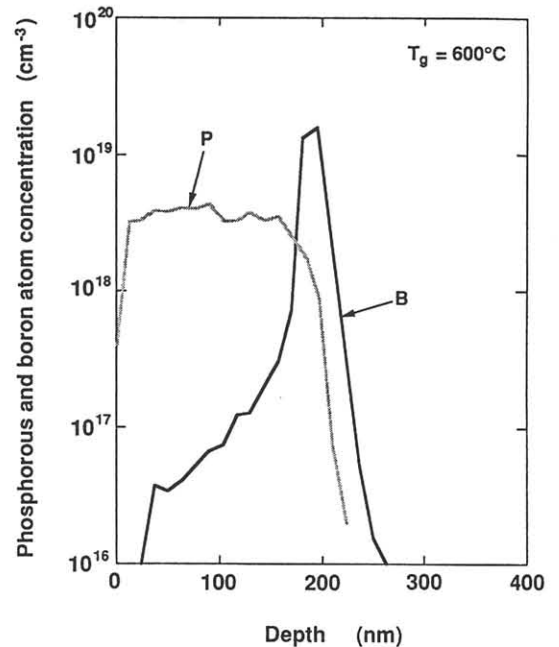


Fig. 4 The profiles of boron and phosphorous atoms in the continuously grown  $p^+-n^+$  photo-epitaxial layer. The doped phosphorous concentration was  $5 \times 10^{18} \text{ cm}^{-3}$ , and the doped boron concentration was  $2 \times 10^{19} \text{ cm}^{-3}$ .

photo-epitaxial layers were extremely abrupt, and no phosphorous atoms were precipitated at the  $n^+$ - $p^+$  interface (Fig. 4).

The surface morphology of the  $n^+$  photo-epitaxial layer grown on the  $p^+$  photo-epitaxial layer with a boron concentration of  $2 \times 10^{19} \text{ cm}^{-3}$  was smooth (Fig. 5(a)). Surprisingly, the surface pits shown in Fig. 3 were not observed, and very specular surface was obtained. At the interface of the  $p^+$  and  $n^+$  photo-epitaxial layers, there was no discontinuous growth or phosphorous precipitation, and both layers had good crystallinity (Fig. 5(b)).

The surface-pits density at the  $n^+$  photo-epitaxial layer surface was strongly concerned with the boron concentration in the  $p^+$  photo-epitaxial layer (Fig. 6). The boron concentration was controlled by the diborane flow rate from  $5 \times 10^{17} \text{ cm}^{-3}$  to  $1 \times 10^{21} \text{ cm}^{-3}$ , and the phosphorous concentration in the  $n^+$  photo-epitaxial layer was held at  $5 \times 10^{18} \text{ cm}^{-3}$ . The surface pit density decreased markedly with increasing the boron concentration. Surface pits completely disappeared at boron concentrations above  $1 \times 10^{19} \text{ cm}^{-3}$ . Above the boron concentration of  $1 \times 10^{20} \text{ cm}^{-3}$ , another defect appeared. This defect was caused by the degradation of crystal quality of the  $p^+$  photo-epitaxial layer because the boron atoms are not completely activated, and degraded the crystal quality above the doped boron concentration of  $1.5 \times 10^{20} \text{ cm}^{-3}$ .

Even though lattice mismatch and stresses at the interface of the  $n^+$ - $p^+$  photo-epitaxial layers are larger than those at the interface of the  $n^+$  photo-epitaxial layer and the  $p^-$  substrate, the surface pit density at the  $n^+$  photo-epitaxial layer grown on the  $p^+$  layer is much smaller than that grown on the  $p^-$  substrate. This phenomenon is deeply related to the hole density at the crystal surface. The high surface hole density apparently decreases hydrogen surface coverage, activating dehydrogenation and surface migration of adsorped species. As a result, phosphorous atoms on the  $p^+$  photo-epitaxial layer are less likely to be precipitated at the initial stage of the  $n^+$  photo-epitaxial growth. The defects density of heavily phosphorous doped photo-epitaxial layer was greatly improved by  $p^+$ - $n^+$  continuous growth.

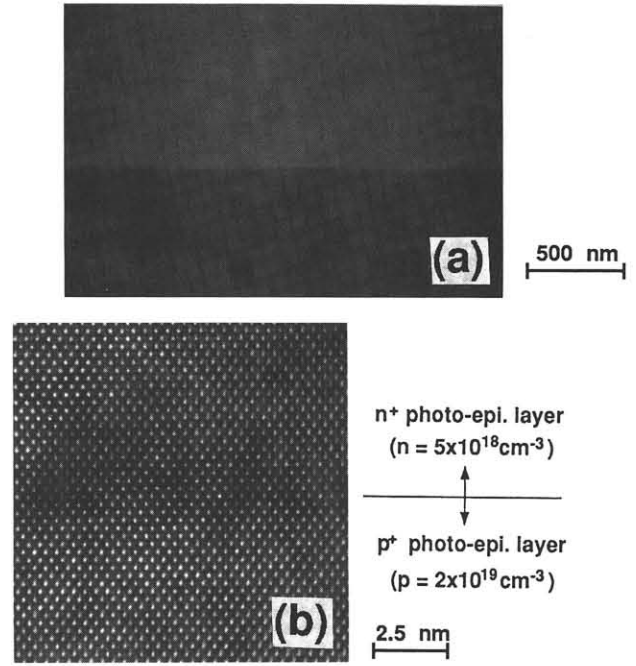


Fig. 5 The  $n^+$ - $p^+$  continuously grown layer. (a) SEM photograph of the surface morphology. (b) TEM photograph of the cross section of the  $n^+$ - $p^+$  interface.

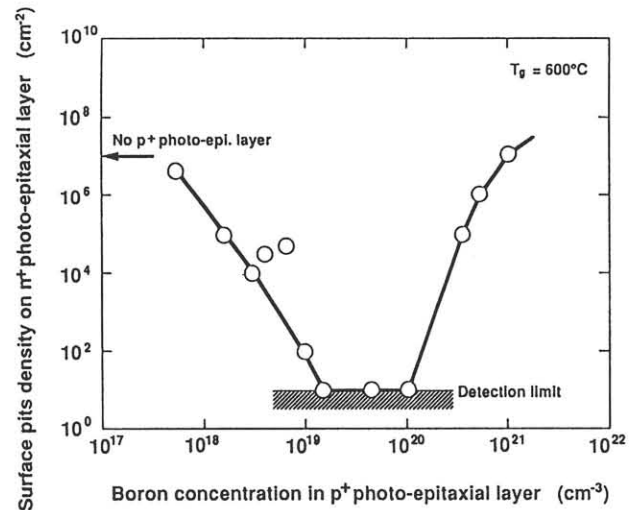


Fig. 6 Boron concentration in the  $p^+$  photo-epitaxial layers and surface pit density at the  $n^+$  photo-epitaxial layer surface.

Table 1 Activation ratio of phosphorous atoms and electron Hall mobility in the  $n^+$  photo-epitaxial layer grown on the  $p^-$  substrate or  $p^+$  photoepitaxial layer. The  $p^-$  substrate has a resistivity of  $10 \Omega\text{cm}$ , and the  $p^+$  photo-epitaxial layer has a boron concentration of  $2 \times 10^{19} \text{ cm}^{-3}$ .

	Photo- $n^+$ / photo- $p^+$ / $p^-$ -sub.	Photo- $n^+$ / $p^-$ -sub.
Phosphorous atom activation ratio	100%	60%
Electron mobility ( $\mu / \mu_0$ )	1.0	0.6

$\mu_0$  : Bulk Si electron mobility

### (3) Electrical properties

The  $n^+$ - $p^+$  continuous growth also greatly improved the crystal quality of the  $n^+$  photo-epitaxial layer. The activation ratio of phosphorous atoms and the electron Hall mobility in the  $n^+$  photo-epitaxial layer grown on the  $p^+$  photo-epitaxial layer or  $p^-$  substrate were determined by Hall measurement and SIMS analysis (Table 1). The phosphorous activation ratio was improved from 60% to 100%, and the electron Hall mobility became the same as that of bulk Si by  $p^+$ - $n^+$  continuous growth.

We measured the I-V characteristics of this  $p^+$ - $n^+$  junction which has a boron concentration of  $2 \times 10^{19} \text{ cm}^{-3}$  and a phosphorous concentration of  $5 \times 10^{18} \text{ cm}^{-3}$  (Fig. 7). The breakdown voltage was about 2.5 V which was limited by the electron concentration in  $n^+$  photo-epitaxial layer, and agrees well with the reported value of the Zenner breakdown.

Using this  $p^+$ - $n^+$  junction, we made a bipolar transistor. This transistor had good  $I_c$ - $V_{ce}$  characteristics and no emitter-collector short (Fig. 8). The  $p^+$ - $n^+$  layers continuously grown by photo-epitaxy have device-level quality.

### Conclusion

We continuously grew a heavily phosphorous doped photo-epitaxial layer with a  $5 \times 10^{18} \text{ cm}^{-3}$  electron concentration on a heavily boron doped photo-epitaxial layer at  $600^\circ\text{C}$ . The impurity profiles of the phosphorous and boron atoms were extremely abrupt. Surface pits on the  $n^+$  photo-epitaxial layer that were caused by the precipitation of phosphorous atoms were greatly decreased by increasing the hole concentration in the  $p^+$  photo-epitaxial layer, and these pits completely disappeared at hole concentrations above  $1 \times 10^{19} \text{ cm}^{-3}$ . This  $n^+$ - $p^+$  continuous growth technique also greatly improved the electrical properties and phosphorous activation ratio in the  $n^+$  photo-epitaxial layer, and realizing the device-level quality. This technique makes it possible to create arbitrary impurity profiles with high crystal quality and new device structures.

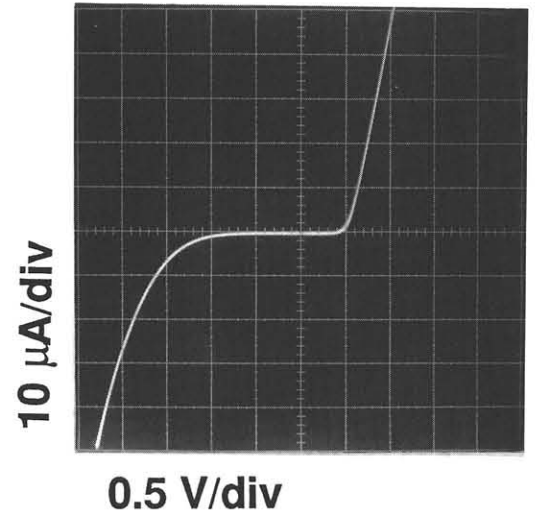


Fig. 7 The I-V characteristic of the  $p^+$ - $n^+$  diode fabricated using  $p^+$ - $n^+$  continuous growth.

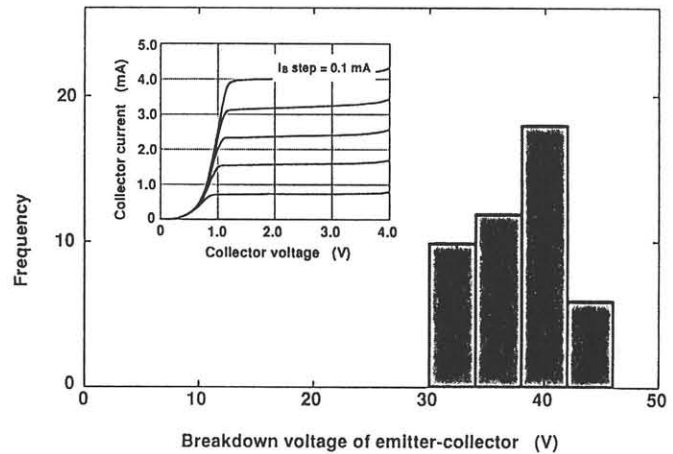


Fig. 8 Distribution of the emitter-collector breakdown voltage and  $I_c$ - $V_{ce}$  characteristics of the bipolar transistor which was made using  $p^+$ - $n^+$  continuously grown layer.

### Acknowledgement

We thank Dr. H. Ishikawa for his encouragement, Mr. U. Kataoka for the SIMS analysis, and Mr. K. Suzuki, T. Fukano and H. Shido for device fabrication.

### Reference

- (1) B. S. Meyerson, *Appl. Phys. Lett.*, **48**, 797 (1986).
- (2) T. J. Donahue et al., *J. Appl. Phys.*, **57**, 2757 (1985).
- (3) S. Nishida et al., *Appl. Phys. Lett.*, **49**, 79 (1986).
- (4) T. Ohmi et al., *Appl. Phys. Lett.*, **52**, 2236 (1988).
- (5) T. Tatsumi et al., *Appl. Phys. Lett.*, **50**, 1234 (1987).
- (6) T. Yamazaki et al., in *Dig. of Tech. Paper of 1984 Symp. on VLSI Technology*, San Diego, 1984, pp. 56-57. (IEEE CAT. No. 84 CH 2061-0).
- (7) T. Yamazaki et al., in *Tech. Dig. of the IEDM*, Washinton, 1987, pp. 586-589 (IEEE CAT. No. 87 CH 2515-5).
- (8) S. Watanabe et al., in *Ext. Abstract of the 20th Conf. on SSDM*, Tokyo, 1986, pp. 117-120.